Journal of the Korean Magnetic Resonance Society **2015**, *19*, 88-94
DOI 10.6564/JKMRS.2015.19.2.088

Structural stability of CD1 domain of human mitotic checkpoint serine/threonine-protein kinase, Bub1

Hyun-Hwi Kim[1], Hyun-Kyu Song[2], Bong-Jin Lee[3*], and Sung Jean Park[1*]

[1] College of Pharmacy, Gachon University, 534-2 Yeonsu-dong, Yeonsu-gu, Incheon, Republic of Korea
[2]School of Life Sciences and Biotechnology, Korea University, Anam-Dong, Seongbuk-Gu, Seoul 136-701, Korea
[3]Research Institute of Pharmaceutical Sciences, College of Pharmacy, Seoul National University, San 56-1, Shillim-Dong, Kwanak-Gu, Seoul 151-742, Korea

Received Aug 16, 2015; Revised Sep 12, 2015; Accepted Sep 20, 2015

Abstract Bub1 is one of the spindle checkpoint proteins and plays a role in recruitment of the related proteins to kinetochore. Here, we studied the structural characteristic of the evolutionarily conserved 160 amino acid region in the N-terminus (hBub1 CD1), using Circular Dichroism (CD) and NMR. Our CD results showed that hBub1 CD1 is a highly helical protein and its structure was affected by pH: as pH was elevated to basic pH, the helical propensity increased. This could be related to the surface charge of the hBub1 CD1. However, the structural change did not largely depend on the salt concentration, though the thermal stability a little increased. The previous NMR analysis[1] revealed that the hBub1 CD1 adopts eight helices, which is consistent with the CD result. Our result would be helpful for evaluating the molecular mechanism of the hBub1 CD1 and protein-protein interactions.

Keywords NMR, CD, Bub1, human mitotic checkpoint serine/threonine-protein kinase

Introduction

The metaphase-to-anaphase transition occurs only after all chromosomes have established bipolar attachment to the mitotic spindle. The spindle checkpoint delays anaphase onset when any kinetochore in the cell is not properly bound with the spindle microtubules or when kinetochores are not under tension normally produced by bipolar attachment.[2,3] Activation of the checkpoint involves kinetochore localization of several spindle checkpoint proteins, including Mad1, Mad2, Bub1, BubR1 (Mad3 in yeast), Bub3, MAPK, and Mps1[4], leading to the complex formation between Mad2, BubR1, Bub3, and Cdc20.[5-8] When sequestered by the checkpoint proteins, Cdc20 is unable to activate the anaphase-promoting complex (APC), an E3 ubiquitin protein ligase that triggers degradation of several mitotic regulators, including the anaphase inhibitor Pds1 (also named securin).[9] Once the spindle checkpoint signal is terminated, Cdc20 is then able to direct APC toward Pds1. Degradation of Pds1 frees the protease Esp1 that in turn cleaves cohesin complex, allowing sister chromatids to separate.[9] In this way, the spindle checkpoint delays anaphase onset until all kinetochores are properly

* Address correspondence to: **Sung Jean Park** or **Bong-Jin Lee,** College of Pharmacy, Gachon University, 534-2 Yeonsu-dong, Yeonsu-gu, Incheon, Republic of Korea, Tel: 82-32-820-6113; E-mail: psjnmr@gachon.ac.kr **for Sung Jean Park** or Research Institute of Pharmaceutical Sciences, College of Pharmacy, Seoul National University, San 56-1, Shillim-Dong, Kwanak-Gu, Seoul, 151-742, Korea, Tel: 82-2-880-7869; Fax: 82-2-872-3632; E-mail: lbj@nmr.snu.ac.kr **for Bong-Jin Lee**

attached to spindle microtubules.

Both Bub1 and BubR1 bind to Bub3 throughout the cell cycle, and the interaction is important for kinetochore localization of all three proteins.[8,10-12] Mad1 binds tightly to Mad2 during interphase and mitosis, and it recruits Mad2 to kinetochores.[13,14] In vertebrate cells, a small fraction of MAPK is activated and enriched at kinetochores during mitosis, and the level of active MAPK at kinetochores decreases at and after metaphase.[15,16] MAPK is important for the spindle checkpoint in egg extracts and in somatic cells.[14,17,18] Bub1 inhibits ubiquitin ligase activity of anaphase promoting complex (APC) preventing mitosis until all chromosomes are correctly attached to the mitotic spindle.

Although Bub1 (Figure 1) is well characterized for its biological activity as a spindle checkpoint component, a structural information is still insufficient to meet our intellectual curiosity. Therefore, this study was aimed to reveal the structural characteristics of Bub1 protein by performing various NMR and circular dichroism (CD) experiments. The purification protocol for this protein was optimized. The secondary structures of Bub1 CD1 and the effect of pH, salt, temperature on the protein structure were evaluated by CD spectroscopy as well as NMR. These findings would make it possible to obtain samples of the Bub1 protein that suitable for structural studies by NMR.

Experimental Methods

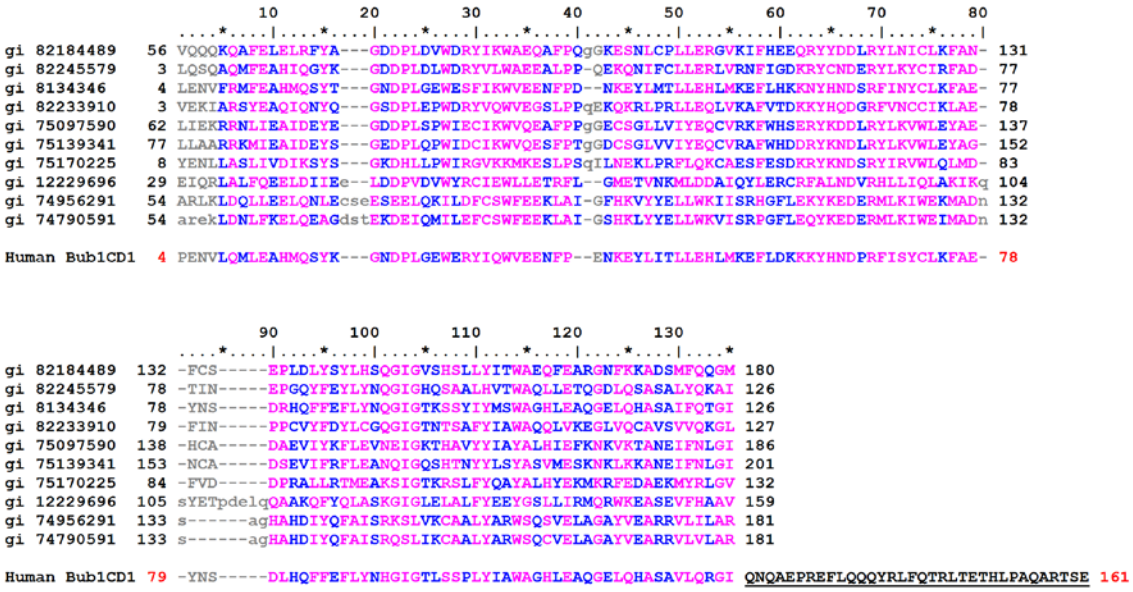

Figure 1. Mad3/BUB1 homology region 1 classified in various organism. This result was obtained from pfam database (pfam 08311.1, Ref). gi 82184489 (Bub1b protein Xenopus laevis, African clawed frog), gi 82245579 (Spindle checkpoint protein Bub1, Xenopus laevis, African clawed frog), gi 8134346 (Mitotic checkpoint serine/threonine-protein kinase BUB1 (MBUB1)), Mus musculus, house mouse), gi 82233910 (Hypothetical protein, Gallus gallus, chicken), gi 75097590 (an expressed protein, Arabidopsis thaliana, thale cress), gi 75139341 (Putative mitotic spindle checkpoint component mad3, Oryza sativa, japonica cultivar-group), gi 75170225 (Arabidopsis thaliana genomic DNA, chromosome 5, Arabidopsis thaliana, thale cress), gi 12229696 (Checkpoint serine/threonine-protein kinase bub1, Schizosaccharomyces pombe, fission yeast), gi 74956291 (Suspended animation (Anoxia-induced) defective protein 1, Caenorhabditis elegans), gi 74790591 (Hypothetical protein CBG12617, Caenorhabditis briggsae). The gray, blue, and red residues are non-conserved, conserved, and highly conserved residues, respectively. The black residues underlined are additional residues of the human Bub1 CD1 domain which were used in this study.

Overexpression of Bub1- *E. coli* BL21 (DE3) transformed with the GST-Bub1 gene expression vector was precultured in LB broth supplemented with kanamycin at 50 μg/ml and transferred to M9 minimal medium using ^{15}N ammonium chloride as the nitrogen source and glucose as the carbon source. For preparing triply [^{15}N, ^{1}H]-labeled Bub1, two liter cultures of the transformed *E.coli* were grown in M9 media with ^{15}N ammonium chloride as the nitrogen source. The BL21(DE3) cells containing Bub1 construct were grown at 37℃ and 170 rpm to an optical density of 0.5~0.6 at 600 nm. Induction of expression was achieved by the addition of a IPTG (to final concentration of 1mM or 0.5mM) and further incubation at 37℃ for 5h. The M9 medium contained vitamin complex. This stock solution should be added to M9 media to a concentration of 1 mL/1L. The induced cells were harvested by centrifugation at 8000 rpm for 15min at 4℃ and were stored at –80℃.

Protein preparation- The supernatant was applied to a Glutathione-Sepharose 4B column (2.5 X 20 cm), which was previously equilibrated with PBS buffer [140mM NaCl, 2.7mM KCl, 10mM Na2HPO4, 1.8mM KH2PO4, 1mM β-mercaptoethanol (BME), pH7.3]. Bound GST- Bub1 was eluted with 50 ml of the elution buffer [30 mM glutathione in 50 mM Tris-Cl, pH 8.0] at the flow rate of 1 ml/min. The fused GST was removed from eluted protein by treating with thrombin at room temperature for 12 hr. After cleavage, the reaction mixture was loaded onto an anion-exchange column (Q-Sepharose) , which was previously equilibrated with buffer [50mM Tris-HCl, 50mM NaCl, 1mM β-mercaptoethanol, 1mM EDTA, 1mM PMSF] and eluted with salt gradient (0~500mM NaCl). The eluted solution was dialyzed overnight against 50 mM Na.phosphate (pH 6.8), 50 mM NaCl, 1 mM EDTA, and 100μM PMSF and stored at 4°C and concentrated using a centriprep and centricon 30 unit (Amicon Inc. Beverly, MA).
To determine the extinction molar coefficient accurate mass of Bub1 was measured using microbalance and its concentration was calculated. The dry Bub1 was dissolved in 5mM sodium phosphate buffer (pH7.4) and then measured the absorbance at 280nm. We calculated extinction molar coefficient employing Beer-Lambert's law. The Bub1 concentration was estimated using the calculated extinction molar coefficient of 1174.98 $M^{-1}cm^{-1}$.

The estimation of the secondary structure of protein - To characterize the secondary structure of the Bub1, CD analysis was performed. All of the CD experiments were performed on a Jasco J-715 spectropolarimeter equipped with a temperature controlling unit, using a 2 mm path-length cell, with a 1 nm bandwidth and 4sec response time. The standard far-UV CD spectra were collected at 20℃ with a scan speed of 50 nm/min and 0.5 nm step resolution. These individual scans taken from 250 to 190 nm were added and averaged, followed by subtraction of the solvent CD signal. All the experiments were repeated three to four times and were reproducible. The Bub1 purified as described above were dialyzed against 50 mM sodium phosphate buffer (pH6.8) and concentrated using a centricon 30 unit. The concentration of protein used in CD measurements was ranged from 10 μM to 30 μM. The resultant spectra were corrected for the buffer signal.
Thermal denatureration was monitored by measuring the CD signals at 222 nm (CD222) with increasing temperature from 20 to 80℃. Basically, the temperature scan rate was manifested at 60℃/h and the CD signal was recorded at every 0.1℃

Structure studies by NMR spectroscopy- NMR spectra were acquired on a Bruker AVANCE 600 MHz spectrometer at 303 K for the best dispersion of resonance. The spectra recorded on ^{15}N-labelled Bub1 were 2D ^{15}N-HSQC. All of the spectra were processed and visualized using the NMRPipe/NMRDraw software[19] and NMRView program.[20]

Results and Discussion

Overexpression and separation of Bub1- Bub1 constructs could be expressed in *E.coli* BL21 (DE3) codon+. The level of overexpression was already checked by SDS-PAGE in the phase of the construction of Bub1, which results are shown Figure 2. The overexpression band was major among the produced bands (so called, 'main band' or 'target band').[21] The target band was thickened remarkably while the others were not increased. This mean that the efficiency of the overexpression of Bub1 was very high and it may be easy to purity the protein without a loss.[22] To acquire the best induction point, the growth curve of cell in the presence or absence of IPTG was checked. As a result of various experiment to find the best condition of induction, the induction time, the final concentration of IPTG (50μg/ml) and culture temperature (37℃) were determined.

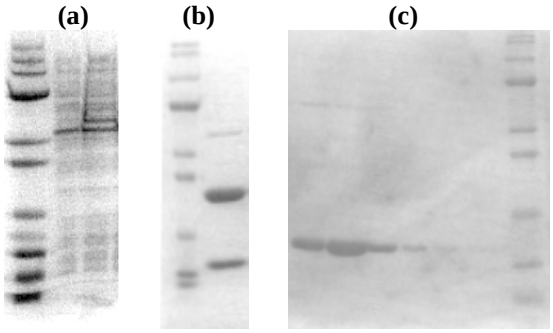

Figure 2. Overexpression of recombinant Bub1 in *E. coli* and the purification of Bub1. (a) The expression was induced in *E. coli* BL21 (DE3) with 0.5 mM IPTG at 37℃ for 4h. Uninduced cells (lane 1), induced cells (lane 2) are shown. (b) The fused GST was removed from eluted protein by treating with thrombin at room temperature for 12 hr. (c) After cleavage, the reaction mixture was purified over an anion-exchange column.

pH and salt dependence of hBub1 CD1 structure: CD study- The hBub1 CD1 is highly ordered in a buffer condition, since the presence of two negative extremes at 222 and 208 nm and the positive intensity below 200 nm point a highly helical conformation adopted by the protein (Fig. 3). Such hBub1 CD1 undergoes showed large structural change in buffer solution when the pH is reduced to 4 or elevated to 8 (Fig. 3a). Absolute values of intensity at 208 nm and 222 nm appear to be higher at pH 8 than at the others. The ratio of 208/222 nm was gradually decreased as pH decreased toward 5 (Fig. 3c), suggesting that the conformational characteristic of the hBub1 CD1 depends on pH.

This structural transition could be related to the change of surface charge property of the protein, since the calculated pI value of the hBub1 CD1 is about 5.3 and the net charge is - 9. In general, various protein-protein interactions depend on their surface charge properties. Thus, it is noteworthy that the structure of the hBub1 CD1 can be easily converted by the charge property. It is probable that the surface charge property of the hBub1 CD1 may regulate the interaction with other protein. Interestingly, CD signal was a little intensified at pH 4, compared that at pH 5 (Fig. 3a) and the ratio of 208/222 nm at pH 4 was almost recovered to that at pH 8 (Fig. 3c). This may suggest that below pH 5 the protein forms a mis-fold or aggregates, which is evidenced by the Tm curve (Fig. 3e). The Tm curve at pH 4 did not show any unfolding transition point, suggesting the fold at lower pH is not compact and not like that of the native state. Except pH 4, Tm curves at various pH, clearly showed that the tertiary structure of the hBub1 CD1 is compact (Fig. 3e); from pH 8 to 6, the hBub1 CD1 showed the discrete melting point about 65 degrees C. In this pH range, the tertiary fold itself seems not to be largely changed while the ratio of 208/222 nm showed big differences. This result could suggest that the hydrophobic core is not highly affected by these pHs. However, near the pI point, that is pH 5, the melting temperature decreased to about 55 degrees C. Tm curve at pH 4, described above, was linear, which is the general characteristic of unordered or loosely folded proteins. Figure 3b shows the effect of ionic strength on the structure of the hBub1 CD1. The curves showed a little difference according to salt concentration. However, on the contrary to the result of pH titration, the salt titration did not show any direct association with concentration, which is clearly shown in figure 3d. The structural stability was also verified by scanning the Tm curves of the hBub1 CD1 with increasing ionic strength. With increasing the salt concentration,

the melting temperature of the hBub1 CD1 slightly increased (Fig. 3f). However, without salt, the slight intensification of CD signal at 222 nm occurred at the initial stage of temperature elevation, indicating that without salt the thermal stability of the hBub1 CD1 decreased and the protein may form aggregates in the solution. Thus, in the wide range of salt concentration, the hBub1 CD1 seems to maintain its tertiary fold at normal pH.

Measurement of ^{1}H, ^{15}N-HSQC spectrum- Next, we examined the effects of temperature change and salt concentrations on the structure of Bub1 using ^{1}H,^{15}N-HSQC spectra since to monitor the HSQC spectrum of a protein is efficient way to figure out the structural changes of the protein (Figure 4). As salt concentration increased, resonance dispersion was not highly affected, of which result is identical to CD data. However, long NMR measurement of the protein in above 300 mM salt concentration provides the precipitation of the hBub1 CD1. In addition, the temperature stability of the hBub1 CD1 was low since the protein precipitated at 40℃.

Concluding Remarks

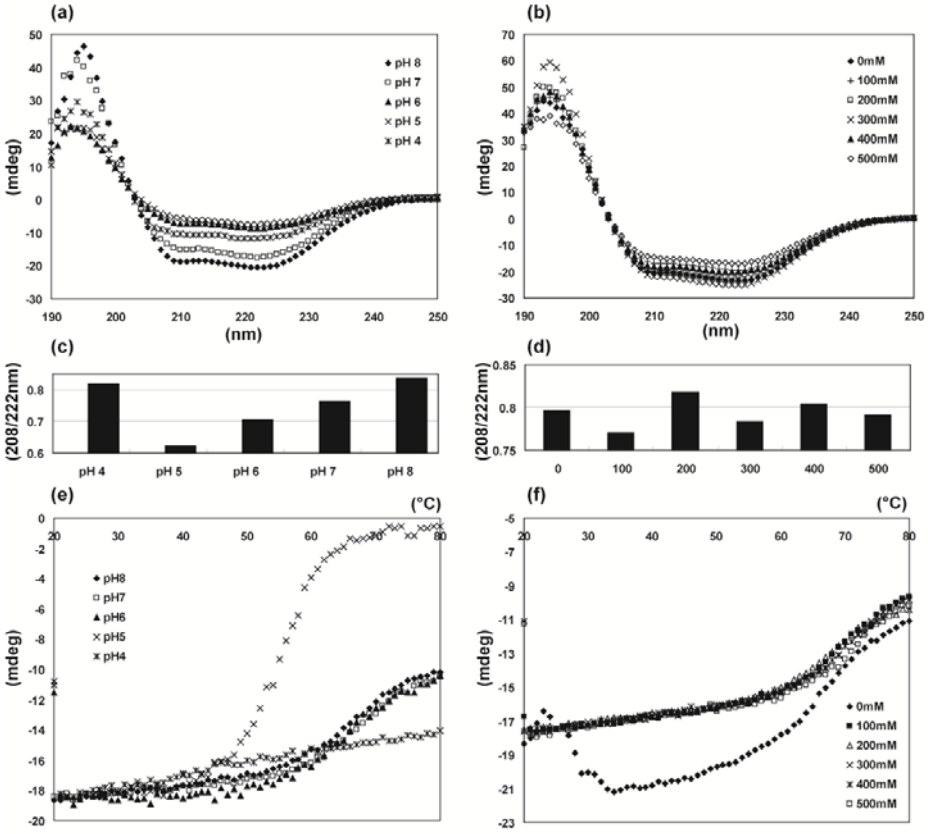

Figure3. CD spectra recorded in 5 mM potassium phosphate buffer supplemented with 50 mM NaCl, 1 mM EDTA and 1 mM DTT. (a) Effect of pH change on the structure of the hBub1 CD1. For pH-titration experiment, pH of each sample was adjusted by 0.1 N HCl. (b) Effect of salt (NaCl) concentration on the structure of the hBub1 CD1 (c) The signal ratio between 202 and 222 nm depending on pH. (d) The signal ratio between 202 and 222 nm depending on slat concentration. (e) Tm curves of the hBub1 CD1 at various pHs. Temperature scan was performed at 222 nm in a temperature range between 20°C and 80°C. (f) The effect of salt (NaCl) concentration on the structural stability was evaluated by observation of shift of Tm value with increasing salt concentration at pH 7.

Previously, we showed first NMR report that the hBub1 CD1 is a highly helical protein and consists of eight helices.[1] The helical propensity was well consistent with the current result of CD and NMR analysis. In addition, the surface charges seem to affect the structural stability and the helical composition of the hBub1 CD1. Our result would be helpful for evaluating the molecular mechanism of the hBub1 CD1 and protein-protein interactions.

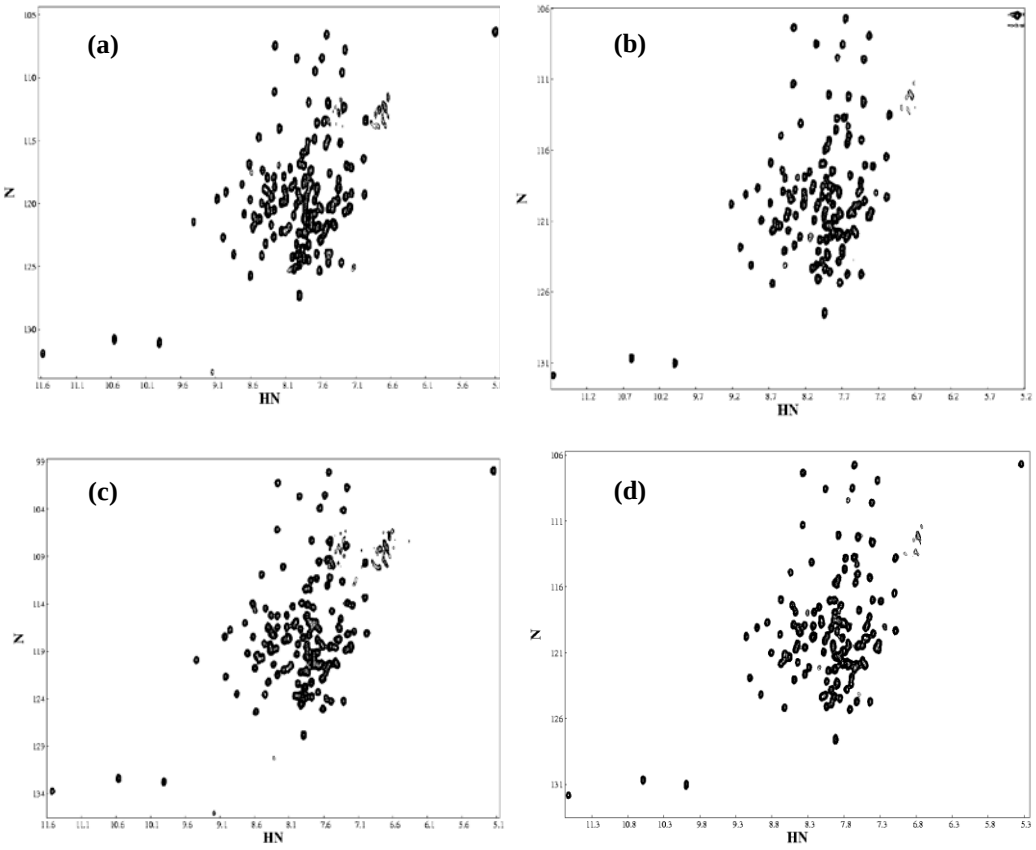

Figure 4. HSQC spectrum of CDI domain of hbub1. Each spectrum was recorded at the condition of (a) 30℃, salt 50mM. (b) 40℃, salt 50mM. (c) 30℃, salt 300mM. (d) 40℃, salt 300mM

Acknowledgements

This research was supported by the Bio & Medical Technology Development Program of the NRF funded by the Korean government, MSIP (NRF-2014M3A9B6069340) and was also supported by the Gachon University Gil Medical Center (Grant number : 2013-36).

References

1. S. J. Park, H.-H. Kim, Y.-S. Jung, S.-J. Kang, H.-K. Cheong, H.-K. Song, and B.-J. Lee, *Biomol NMR Assign* **6**, 109 (2012)
2. X. Li and R. B. Nicklas, *Nature.* **373**, 630 (1995)
3. C. L. Rieder, R. W. Cole, A. Khodjakov, and G. Sluder, *J. Cell. Biol.* **130**, 941 (1995)
4. D. W. Cleveland, Y. Mao, and K. F. Sullivan, *Cell.* **112**, 407 (2003)
5. K. G. Hardwick, R. C. Johnston, D. L. Smith, and A. W. Murray, *J. Cell. Biol.* **148**, 871 (2000)
6. R. Fraschini, A. Beretta, L. Sironi, A. Musacchio, G. Lucchini, and S. Piatti, *EMBO. J.* **20**, 6648 (2001)
7. Y. Zhang and E. Lees, *Mol. Cell. Biol.* **21**, 5190 (2001)
8. R. H. Chen, *J. Cell. Biol.* **158**, 487 (2002)
9. J. M. Peters, *Mol. Cell.* **9**, 931 (2002)
10. J. Basu, E. Logarinho, S. Herrmann, H. Bousbaa, Z. Li, G. K. Chan, T. J. Yen, C. E. Sunkel, and M. L. Goldberg, *Chromosoma.* **107**, 376 (1998)
11. S. S. Taylor, E. Ha, and F. McKeon, *J. Cell Biol.* **142**, 1 (1998)
12. H. Sharp-Baker and R. H. Chen, *J. Cell. Biol.* **153**, 1239 (2001)
13. R. H. Chen, A. Shevchenko, M. Mann, and A. W. Murray, *J. Cell. Biol.* **143**, 283 (1998)
14. E. Chung and R. H. Chen, *Mol. Biol. Cell.* **13**, 1501 (2002)
15. P. S. Shapiro, E. Vaisberg, A. J. Hunt, N. S. Tolwinski, A. M. Whalen, J. R. McIntosh, and N. G. Ahn, *J. Cell. Biol.* **142**, 1533 (1998)
16. M. Zecevic, A. D. Catling, S. T. Eblen, L. Renzi, J. C. Hittle, T. J. Yen, G. J. Gorbsky, and M. J. Weber, *J. Cell. Biol.* **142**, 1547 (1998)
17. J. Minshull, H. Sun, N. K. Tonks, and A. W. Murray, *Cell.* **79**, 475 (1994)
18. X. M. Wang, Y. Zhai, and J. E. Ferrell, *J. Cell. Biol.* **137**, 433 (1997)
19. F. Delaglio, S. Grzesiek, G. W. Vuister, G. Zhu, J. Pfeifer, and A. Bax, *J. Biomol. NMR.* **6**, 277 (1995)
20. B. A. Johnson and R. A. Blevins, *J. Biomol. NMR.* **4**, 603 (1994)
21. S. J. Park, *J. Korean Magn. Reson. Soc.* **18**, 47 (2014)
22. S.-J. Hur, H.-W. Lee, A.-H. Shin, and S. J. Park, *J. Korean Magn. Reson. Soc.* **18**, 10 (2014)